PCCP

PAPER

View Article Online
View Journal | View Issue

Cite this: *Phys. Chem. Chem. Phys.*, 2015, **17**, 6572

Promoting the "water-wire" mechanism of double proton transfer in [2,2′-bipyridyl]-3,3′-diol by porous gold nanoparticles

Tarak Nath Nag, Tarasankar Das, Somen Mondal, Arnab Maity and Pradipta Purkayastha*

Received 4th September 2014,
Accepted 21st January 2015

DOI: 10.1039/c4cp03968h

www.rsc.org/pccp

The effect of nanopores in porous gold nanoparticles (Au NPs) on excited-state double proton transfer (DPT) in [2,2′-bipyridyl]-3,3′-diol ($BP(OH)_2$) in an aqueous environment is the main focus of the present work. DPT in $BP(OH)_2$ is known to take place through two mechanisms. In a bulk environment, an open solvated molecule facilitates the process and emits at 460 nm whereas, in a confined situation, formation of a "water wire" between the prototropic centers leads to the transfer of protons. It has been shown spectroscopically in the present study that in the nanovessels provided by nanoporous Au NPs, the unconventional mechanism of DPT through the formation of a "water wire" is promoted due to the presence of a limited number of water molecules around the probe. Experiments in the presence of solid pure Au, Ag and Au/Ag NPs were performed to support our proposition. Time-resolved fluorescence spectral changes confirm our findings.

1. Introduction

It is now well known that proton transfer plays important roles in chemistry and biology. Ground- and excited-state proton transfers have become important from the mechanistic point of view.[1–6] Single and double proton transfer probes are quite well known and serve as important and interesting means to discover many chemical and biological consequences. For a long time, double proton transfer (DPT) has drawn the attention of many in the scientific world.[7–9] In this context, [2,2′-bipyridyl]-3,3′-diol ($BP(OH)_2$) has been considered to be a classical probe. Bulska *et al.* were one of the first groups to report about single and double proton transfer in $BP(OH)_2$.[10,11] According to experimental findings, it was determined theoretically that only one single tautomeric form of $BP(OH)_2$ exists in both the ground state (di-enol form) and the lowest excited singlet state (di-keto form), respectively.[12] In another report on sub-picosecond proton transfer dynamics in $BP(OH)_2$, it was mentioned that the emissive keto-enol tautomeric form of the compound develops in the excited state through a stepwise proton transfer mechanism.[13,14] Studies on DPT in $BP(OH)_2$ were recently carried out extensively by Abou-Zied in different solvents and confined nanocavities of cyclodextrins (CDs).[15,16] In accordance with the previous studies, it was observed that a di-zwitterion (DZ) tautomer is produced in the excited state after intramolecular DPT. The results indicate that the tautomers are sensitive to solvent polarity.[15,16] Further experiments were performed on the binding of $BP(OH)_2$ with ionic and neutral surfactants,[17] Nafion membranes,[18] proteins,[19,20] and lipid vesicles.[21] DPT dynamics were also studied in nanocavities of different forms, such as in cyclodextrins (CDs),[15] molecular sieves of $AlPO_4$-5,[22] and molecular containers of cucurbituril.[23] $BP(OH)_2$ is reported to be devoid of any aqueous solvation inside cucurbituril-7, hence promoting concerted DPT, whereas the surrounding water molecules inside β-CD lead to sequential DPT in $BP(OH)_2$.[23]

Abou-Zied has explained in one of his reports that a special photoinduced tautomerization mechanism takes place in water *via* a "water wire" that connects both of the two hydrogen-bonding centres of the molecule.[16] Proton transfer in this manner is very similar to that explained by the Grotthuss mechanism.[24,25] Theoretical studies on the mechanism and dynamics of DPT through hydrogen-bonded bridging water in a "water wire" show that all molecules hydrogen-bonded to the water wire reduce the tunnelling coefficients of DPT and transfer protons near the transition state.[26] Proton transfer through a "water wire" is extremely important in biology and the phenomenon readily takes place in proteins.[27,28]

In the present report, we have developed a nanoporous gold nanoparticulate surface by dealloying Au/Ag alloy nanoparticles (NPs) and shown that the "water wire" mechanism is promoted for DPT in $BP(OH)_2$ confined in the nanopores. The findings were compared with the effects of pure Au and Ag NPs and Au/Ag

Department of Chemical Sciences, Indian Institute of Science Education and Research (IISER) Kolkata, Mohanpur 741246, India. E-mail: pradiptp@gmail.com; Fax: +91 33 25873020; Tel: +91 33 2587 3019

alloy NPs on DPT in $BP(OH)_2$. The results confirmed the remarkable superiority of the porous Au NPs in promoting the "water wire" mechanism for DPT in $BP(OH)_2$. The unique properties of porous materials develop due to their very high surface-to-mass ratio along with a high adsorption capacity.[29,30]

2. Experimental section

2.1 Materials

Silver nitrate ($AgNO_3$), chloroauric acid trihydrate ($HAuCl_4{\cdot}3H_2O$), sodium borohydride ($NaBH_4$), sodium citrate ($Na_3C_6H_5O_7$) and (2,2-bipyridyl)-3,3-diol were purchased from SDFCL Mumbai, Sigma and Merck, Germany. Methanol and 70% nitric acid (HNO_3) were purchased from Merck, India. Triple-distilled water was used throughout the experiment and all chemicals were used without further purification. A neutral pH of all experimental solutions was carefully maintained.

2.2 Instruments

The absorption spectra were recorded on a Cary 300 Bio UV-vis spectrophotometer and fluorescence measurements were taken using a QuantaMaster 40 spectrofluorometer from Photon Technology International, Inc. The fluorescence lifetimes were measured by the method of time-correlated single photon counting (TCSPC) on a picosecond spectrofluorometer from Horiba Jobin Yvon IBH equipped with a FluoroHub single photon counting controller, Fluoro3PS precision photomultiplier power supply and FC-MCP-50SC MCP-PMT detection unit. The source of excitation was a 340 nm LED with <1 ns time resolution. Atomic force microscopy (AFM) was performed using an NT-MDT NTEGRA instrument procured from NT-MDT, CA, USA. TEM measurements were carried out in a CM 12 (Philips) TEM.

2.3 Synthesis of silver, gold and Au–Ag alloy nanoparticles

Au/Ag NPs were synthesized following a procedure published elsewhere.[31] In brief, Au/Ag alloy NPs were synthesized by varying the initial Au/Ag molar ratios (0 : 1, 0.5 : 0.5, and 1 : 0). The synthesis was performed by reducing $HAuCl_4$ and $AgNO_3$ with $NaBH_4$ in the presence of sodium citrate. The concentration of the metal salts was chosen in such a way that the reaction quotient (Q) was 2.5×10^{-11}, which is below the solubility product (K_{sp}) of AgCl(s), 1.77×10^{-10}.

In three clean 50 mL flasks, 20 mL H_2O and 10 μL 0.01 M sodium citrate were taken. Varying mole fractions of 0.01 M $HAuCl_4$ and 0.01 M $AgNO_3$ were added to each of the solutions to achieve a final metal salt concentration of 5 μM. 10 μL freshly prepared 0.01 M $NaBH_4$ was added to the flasks all at once with vigorous stirring. The solution was allowed to stir for an additional 30 s. A faint colour change occurred almost immediately. The formation of pure Ag, Au and Au/Ag alloy NPs was confirmed from UV-visible spectroscopic analysis. Pure Ag and Au NPs show characteristic absorption peaks at 406 nm and 525 nm, respectively, whereas Au/Ag alloy NPs absorb at 473 nm in an aqueous medium (Fig. 1A).[31]

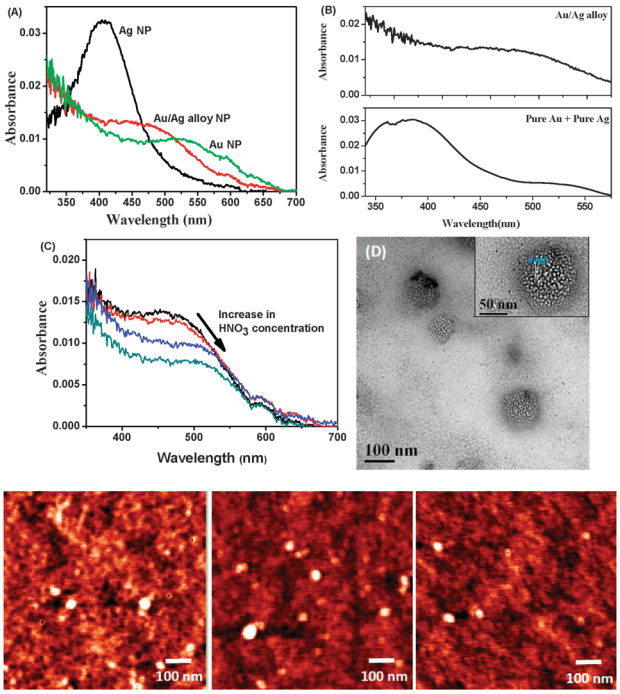

Fig. 1 Formation and characterisation of porous Au NPs from Au/Ag alloy NPs: (A) comparison of absorption spectrum of Au/Ag alloy NP with those of pure Au and Ag NPs; (B) absorption spectrum of Au/Ag alloy NP (upper panel) and mixture of 50% (v/v) pure Au and Ag NPs; (C) demonstration of generation of pores due to addition of dilute HNO_3; (D) HR-TEM image of porous NPs (inset shows pore size); and (lowest panel) (from left to right) AFM images of synthesised Au NPs, Ag NPs and porous Au NPs.

We compared the absorption spectra of the alloy NPs with a mixture of 50% (v/v) pure Ag and Au NPs that produces two distinctly separated peaks at 390 and 523 nm corresponding to the absorbances of pure Ag and Au, respectively (Fig. 1B). To synthesize porous Au NPs, we dealloyed the Au/Ag alloy NPs with dilute HNO_3.[32] On addition of HNO_3 to the alloy NPs, the plasmon peak shifted from 473 nm to 510 nm, clearly indicating that, during addition of the acid, Ag atoms in the alloy were oxidized to Ag^+ ions that, in turn, came out of the alloy NPs, creating pores (Fig. 1C). Along with Ag^+, some Au^{3+} may also have been eliminated from the alloy NPs. Since the standard reduction potential of Au^{3+}/Au is 1.52 V, which is much higher than that of Ag^+/Ag (0.799 V), Ag is more easily oxidized to Ag^+ than is Au to Au^{3+}. The formation of porous NPs was confirmed by absorption spectroscopy and high-resolution transmission electron microscopy (HR-TEM) (Fig. 1D). The diameter of the NPs was measured by atomic force microscopy (AFM) and found to be around 60 nm (Fig. 1, lowest panel). HR-TEM analysis of the porous NPs indicates well-distributed 3 nm-sized pores (Fig. 1D).

3. Results and discussion

3.1 Ground-state behaviour of $BP(OH)_2$ in different nanoparticle environments

The absorption spectrum of $BP(OH)_2$ in water shows a peak at around 344 nm due to transition to the lowest $^1(\pi\pi^*)$ state of

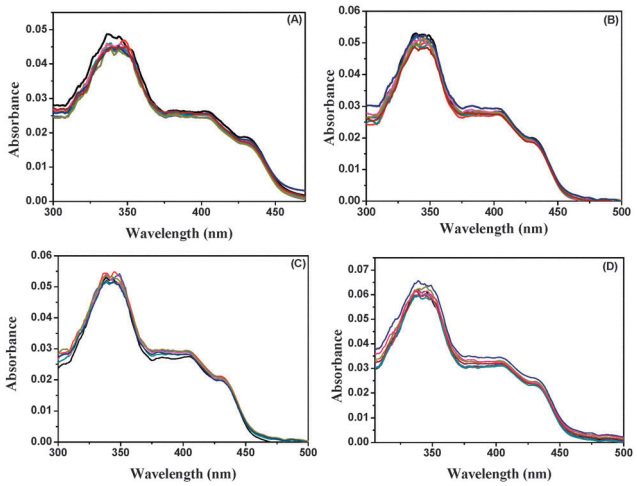

Fig. 2 Absorption spectra of $BP(OH)_2$ with increase in concentration of (A) Ag NPs, (B) Au NPs, (C) Au/Ag alloy NPs, and (D) porous Au NPs. The probe concentration was 4.5 μM.

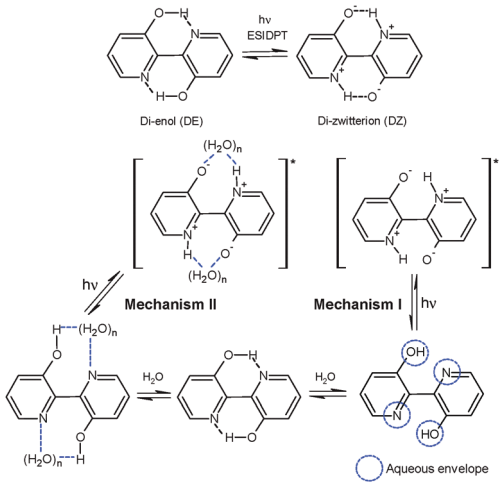

Scheme 1 Tautomerisation of $BP(OH)_2$ and the two most probable mechanistic pathways of tautomerisation of $BP(OH)_2$ in water.

the DE tautomer and the two peaks at around 400 to 450 nm are due to intermolecular hydrogen bonds with the surrounding water molecules.[15] These peaks do not appear in aprotic solvents, nor in hydrophobic pockets.[15,16,23] No appreciable change in the absorption spectrum of $BP(OH)_2$ was observed in either pure Au, Ag and Au/Ag alloys or the porous NPs (Fig. 2). This indicates that water molecules and the DE tautomer coexist under all circumstances.

On explaining DPT in $BP(OH)_2$ in solvents of different polarity and cyclodextrins (CDs), Abou-Zied proposed that the phenomenon may take place through two different mechanisms, as shown in Scheme 1.[16] Mechanism I involves interaction of water molecules with each polar part in $BP(OH)_2$, leading to enol deprotonation and imine protonation to produce the DZ tautomer. In a subsequent work, contradicting his previous report,[15] Abou-Zied mentioned that DZ tautomer formation takes place in the ground state that absorbs in the 400–450 nm region.[16] However, absorption of the hydrogen-bonded prototropic centres of $BP(OH)_2$ with surrounding water molecules before tautomerization seems to be more realistic. Hence, we have changed the schematic (Scheme 1) slightly from that proposed by Abou-Zied.[16] We propose that DPT takes place in the excited state in both mechanisms.

Mechanism II in Scheme 1 shows a different DPT pathway through the formation of a "water wire" between the prototropic centres in the DE tautomer in the ground state. This solvation pattern produces the DZ tautomer in the excited state following a relay transfer of protons through the water wire. As described previously, due to strong solvation of the polar groups by the "water wire" between both hydrogen-bonding centres, the DZ tautomer may exhibit restricted rotation around the central bond between the two aromatic rings.[16]

3.2 Effect of different nanoparticle environments on the excited state of $BP(OH)_2$

$BP(OH)_2$ emits at 460 nm on excitation at 340 nm. This is the emission from the DZ tautomer that forms in the excited state.[15–21] However, numerous works have been reported on DPT in $BP(OH)_2$ and the main focus everywhere was on the behaviour of the 460 nm peak. Abou-Zied first pointed out the appearance of the low-wavelength weak band at 425 nm when he used a β-CD host to encapsulate $BP(OH)_2$. This was explained as appearing due to DPT through the less favoured Mechanism II.[16] This band is at a lower wavelength than that due to Mechanism I because of the restricted rotation of the water-bridged form of $BP(OH)_2$.[16]

Fig. 3 presents the emission spectra of $BP(OH)_2$ with an increase in the concentration of the different solid and porous NPs. It is clearly observed that both mechanisms of DPT in $BP(OH)_2$ are followed in all cases. It is interesting to note that for the solid pure and alloy NPs we observed a slight promotion of Mechanism II at the expense of Mechanism I. The number of water molecules is reduced at the interface of the NPs, which somewhat supports Mechanism II of DPT in $BP(OH)_2$. The effect is overwhelming in the case of porous NPs, where we see a

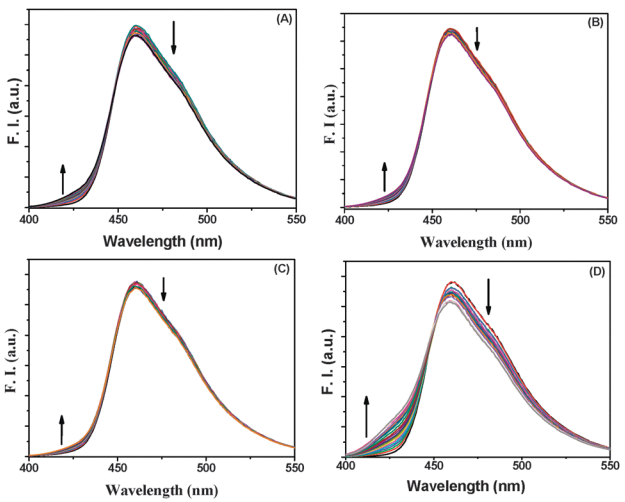

Fig. 3 Emission spectra of $BP(OH)_2$ with increase in concentration of (A) Ag NPs, (B) Au NPs, (C) Au/Ag alloy NPs, and (D) porous Au NPs. The probe concentration was 4.5 μM and the excitation wavelength was 340 nm.

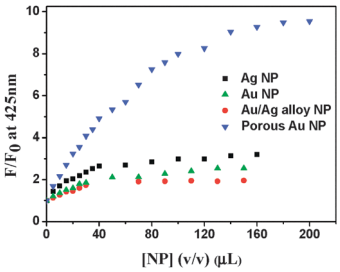

Fig. 4 Relative increase in emission intensity of $BP(OH)_2$ at 425 nm in the presence of the different nanoparticles. The data were taken from the emission spectra in Fig. 3.

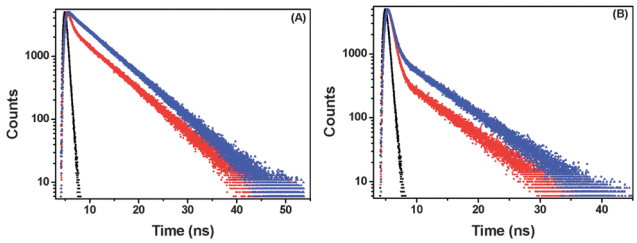

Fig. 6 Time-resolved emission of $BP(OH)_2$ in the absence (red) and presence (blue) of porous Au NPs; the excitation wavelength is 340 nm and the monitored emission wavelengths are (A) 425 nm and (B) 460 nm. The black data are for the prompt.

remarkably high promotion of Mechanism II. The relative effects of the different NPs on DPT in $BP(OH)_2$ are provided in Fig. 4 for better understanding. It is observed that there is nearly a fivefold increase in the possibility of Mechanism II through the formation of a ''water wire''. The results clearly indicate that tautomerization in $BP(OH)_2$ through Mechanism II may be promoted in the presence of a limited number of water molecules around the probe. To consolidate our view, we focused our study on the development of the band at 425 nm on addition of porous Au NPs to the aqueous medium, which appears due to a confined aqueous environment.[16] The nanopores on the surface of the NPs provide numerous nanovessels that can trap guest molecules, along with some water molecules. An increase in the concentration of the porous NPs in solution results in a noticeable enhancement in the intensity of the 425 nm band at the expense of that at 460 nm (Fig. 3D). Hence, it can be presumed that Mechanism II is reinforced inside the Au nanopores.

To confirm that DPT in $BP(OH)_2$ takes place in the excited state in water, we collected the excitation spectra with an increase in the concentration of the porous Au NPs (Fig. 5). The excitation spectrum of $BP(OH)_2$ showed the emergence of a new band at 375 nm at the expense of those between 400 and 450 nm when the 460 nm emission was monitored. The emergence of the new band at 375 nm is also observed in the presence of the solid NPs. This corroborates the description in the previous section. The effect of the porous NPs is overwhelmingly high compared to the other cases. Hence, the new band at 375 nm can be assigned to DPT in $BP(OH)_2$ due to Mechanism II. Such changes were not observed in the absorption spectra. So this also confirms that the DPT phenomenon in the present probe is an excited-state process.

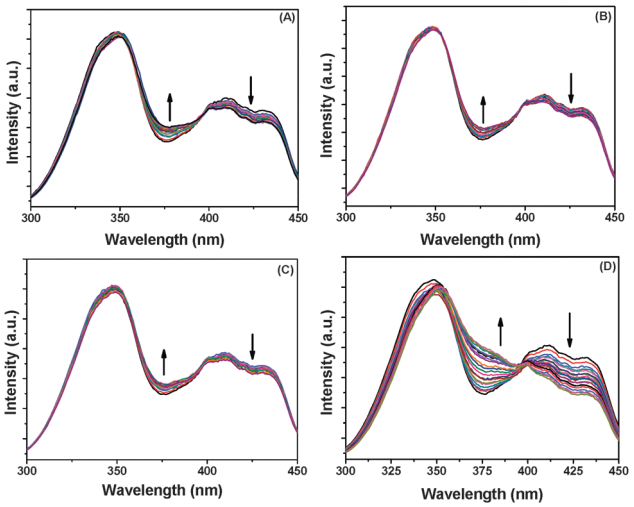

Fig. 5 Excitation spectra of $BP(OH)_2$ with increase in concentration of (A) Ag, (B) Au, (C) Au/Ag alloy, and (D) porous Au NPs. The 460 nm emission was monitored.

3.3 Time-resolved spectral analysis

Time-resolved fluorescence studies were performed to obtain the decay times and contributions of the responsible species in porous NPs. Both 425 nm and 460 nm emissions were monitored. The data could be fitted with a two-exponential function in each case, indicating the coexistence of two emitting species. The decay profiles and parameters are given in Fig. 6 and Table 1, respectively. The shorter-lifetime component (τ_1) is due to the species obtained through Mechanism I and the longer one (τ_2) is because of that produced through Mechanism II as described previously by Abou-Zied.[16] The contribution of the water-wired $BP(OH)_2$ is observed to be more than that of its open counterpart when monitored at 425 nm. Similar circumstances occur on monitoring the 460 nm emission. This clearly indicates the existence of two distinct species in solution. In the porous NPs, monitoring the 425 nm emission shows that the contribution of the shorter-lifetime component decreases significantly, along with an even faster decay, indicating that Mechanism II is favoured in this case. This is also reflected when the 460 nm emission is monitored, where we find that the contribution from the longer-lifetime species increases substantially.

Table 1 Time-resolved fluorescence decay parameters for $BP(OH)_2$ in the absence and presence of porous Au NPs. Values in parentheses indicate the percentage contribution of the individual emitting components. χ^2 values dictate the goodness of the fits to the raw data

λ_{ex} (nm)	λ_{em} (nm)		τ_1 (ps)	τ_2 (ns)	χ^2
340	425	Blank	540 (17%)	6.40 (83%)	1.03
		Porous NPs	440 (3%)	6.40 (97%)	1.06
340	460	Blank	560 (66%)	6.30 (34%)	1.00
		Porous NPs	560 (44%)	6.37 (56%)	1.00

4. Conclusions

DPT in $BP(OH)_2$ was studied in an aqueous medium in the presence of porous Au NPs. It is known that the process takes place in the excited state in water through two different mechanisms. These mechanisms stem from the different solvation characteristics of the probe by water molecules. In one category of solvation, water molecules solvate both of the prototropic centres in the compound and an open structural form develops. In the other type, a "water wire" is created between both of the two centers responsible for proton transfer in $BP(OH)_2$. The second mechanism becomes predominant with lower availability of water molecules around the probe. We find from our study that the nanopores of porous NPs provide nanovessels, where the limited number of water molecules promotes DPT in $BP(OH)_2$ through formation of a "water wire" between the prototropic centers. The suppositions have been clarified by comparing the phenomenon of DPT in the presence of solid Au, Ag and Au/Ag alloy NPs.

Acknowledgements

Financial support from the Department of Science and Technology (SR/S1/PC-35/2011) is gratefully acknowledged. TN thanks IISER Kolkata for support; TD, SM and AM acknowledge the Council of Scientific and Industrial Research and University Grants Commission for their fellowships. The authors are grateful to IIT Kharagpur for the TEM facility.

Notes and references

1 S. Y. Park, O. H. Kwon, T. G. Kim and D. J. Jang, *J. Phys. Chem. C*, 2009, **113**, 16110–16115.
2 Y. Arasaki, K. Yamazaki, M. T. N. Varella and K. Takatsuka, *Chem. Phys.*, 2005, **311**, 255–268.
3 S. Y. Park, Y. S. Lee and D. J. Jang, *Phys. Chem. Chem. Phys.*, 2011, **13**, 3730–3736.
4 L. G. Arnaut and S. J. Formosinho, *J. Photochem. Photobiol., A*, 1993, **75**, 1–20.
5 L. G. Arnaut and S. J. Formosinho, *J. Photochem. Photobiol., A*, 1993, **75**, 21–48.
6 S. K. Mondal, S. Ghosh, K. Sahu, P. Sen and K. Bhattacharyya, *J. Chem. Sci.*, 2007, **119**, 71–76.
7 J. C. Hargis, E. Vöhringer-Martinez, H. L. Woodcock, A. Toro-Labbé and H. F. Schaefer, *J. Phys. Chem. A*, 2011, **115**, 2650–2657.
8 H. Lim, S. Y. Park and D. J. Jang, *Photochem. Photobiol.*, 2011, **87**, 766–771.
9 O. H. Kwon and A. H. Zewail, *Proc. Natl. Acad. Sci. U. S. A.*, 2007, **104**, 8703–8708.
10 H. Bulska, *Chem. Phys. Lett.*, 1983, **98**, 398–402.
11 H. Bulska, A. Grabowska and Z. R. Grabowski, *J. Lumin.*, 1986, **35**, 189–197.
12 A. L. Sobolewski and L. Adamowicz, *Chem. Phys. Lett.*, 1996, **252**, 33–41.
13 H. Zhang, P. van der Meulen and M. Glasbeek, *Chem. Phys. Lett.*, 1996, **253**, 97–102.
14 F. Plasser, M. Barbatti, A. J. A. Aquino and H. Lischka, *J. Phys. Chem. A*, 2009, **113**, 8490–8499.
15 O. K. Abou-Zied, *J. Photochem. Photobiol., A*, 2006, **182**, 192–201.
16 O. K. Abou-Zied, *J. Phys. Chem. B*, 2010, **114**, 1069–1076.
17 D. De and A. Datta, *J. Phys. Chem. B*, 2011, **115**, 1032–1037.
18 E. S. S. Iyer and A. Datta, *J. Phys. Chem. B*, 2012, **116**, 5302–5307.
19 O. K. Abu-Zied, *J. Phys. Chem. B*, 2007, **111**, 9879–9885.
20 D. De, K. Santra and A. Datta, *J. Phys. Chem. B*, 2012, **116**, 11466–11472.
21 P. Ghosh, A. Maity, T. Das, S. Mondal and P. Purkayastha, *Soft Matter*, 2013, **9**, 8512–8518.
22 K. Rurack, K. Hoffmann, W. Al-Soufi and U. Resch-Genger, *J. Phys. Chem. B*, 2002, **106**, 9744–9752.
23 K. Gavvala, A. Sengupta, R. K. Koninti and P. Hazra, *Phys. Chem. Chem. Phys.*, 2014, **16**, 933–939.
24 X. L. Hu, J. Klimeš and A. Michaelides, *Phys. Chem. Chem. Phys.*, 2010, **12**, 3953–3956.
25 A. Hassanali, F. Giberti, J. Cuny, T. D. Kühne and M. Parrinello, *Proc. Natl. Acad. Sci. U. S. A.*, 2013, **110**, 13723–13728.
26 B. K. Mai, K. Park, M. P. T. Duong and Y. Kim, *J. Phys. Chem. B*, 2013, **117**, 307–315.
27 S. Narayan, D. L. Wyatt, D. S. Crumrine and S. Cukierman, *Biophys. J.*, 2007, **93**, 1571–1579.
28 E. Freier, S. Wolf and K. Gerwert, *Proc. Natl. Acad. Sci. U. S. A.*, 2011, **108**, 11435–11439.
29 T. Limnell, J. Riikonen, J. Salonen, A. M. Kaukonen, L. Laitinen, J. Hirvonen and V. P. Lehto, *Int. J. Pharm.*, 2007, **343**, 141–147.
30 H. A. Santos, J. Riikonen, J. Salonen, E. Mäkilä, T. Heikkilä, T. Laaksonen, L. Peltonen, V. P. Lehto and J. Hirvonen, *Acta Biomater.*, 2010, **6**, 2721–2731.
31 M. P. Mallin and C. J. Murphy, *Nano Lett.*, 2002, **2**, 1235–1237.
32 J. Cheng, R. Bordes, E. Olsson and K. Holmberg, *Colloids Surf., A*, 2013, **436**, 823–829.